

https://doi.org/10.1070/QEL17205

Effect of hydrothermal synthesis conditions on up-conversion luminescence intensity of β-$NaYF_4$:Er^{3+}, Yb^{3+} submicron particles

E.A. Sagaidachnaya, Ju.G. Konyukhova, N.I. Kazadaeva, A.A. Doronkina, I.Yu. Yanina, A.A. Skaptsov, A.B.Pravdin, V.I. Kochubey

Abstract. **The differences in the luminescence intensities of up-conversion β-$NaYF_4$:Er^{3+}, Yb^{3+} particles synthesised by the hydrothermal method under various synthesis conditions are studied. The results of the study lead to the conclusion that in order to achieve the maximum luminescence intensity in such particles, it is necessary to use ammonium fluoride and a medium with pH = 3. In this case, the length of the particles increases, up to the formation of rod-shaped particles. Based on the data on the size of the coherent scattering region and on microstresses, we can assume that the particles are polycrystals. At the same time, limiting the size of the coherent scattering region is possible due to the defective structure. When the nanoparticles are synthesised in a medium with pH = 3, hydrolysed regions containing OH groups are formed on the crystallite surface. The presence of these groups does not affect the intensity of up-conversion luminescence of submicron-size particles.**

Keywords: *up-conversion particles, luminescence spectra, Raman scattering.*

1. Introduction

Up-conversion particles with an admixture of lanthanide ions are now becoming increasingly popular because of the prospect of their use in biology and medicine as multimodal probes [1, 2]. The advantages of such particles are obvious. Excitation in the near-IR region of the spectrum, i. e., in the transparency window of biological tissues, ensures the absence of biotissue autofluorescence, a deeper penetration of exciting radiation into biological tissues compared to visible radiation, the absence of photobleaching, etc. [3].

At present, one of the most common crystalline matrices of up-conversion particles is sodium yttrium fluoride $NaYF_4$ [4–6]. In the synthesis of small up-conversion particles that meet the requirements of *in vivo* application [5], one of the main problems is the production of particles with a high quantum yield. It is well known that the efficiency of up-conversion luminescence is influenced by many parameters: size, morphology, phase of the crystal lattice and degree of crystallinity of the particles, concentration of the dopant, type of ions on the particle surface, phonon energy of the crystal lattice, parameters of interaction with the environment, intensity of the exciting radiation, and temperature of the particles [7–9]. For example, a decrease in the particle size to nanometres leads to a decrease in the efficiency of up-conversion [10]. Experiments show that the hexagonal crystal lattice of the matrix allows one to obtain a higher up-conversion luminescence intensity than the cubic one [11]. Besides, an optimum concentration of doping erbium ions was found in the range of 1–2 mol% [12, 13].

The luminescent properties of particles are also affected by the surface state [14], which is mainly due to nonradiative transfer of excitation energy to the environment through high-frequency vibrational modes of ligands, for example, OH, bound to the particle surface.

Currently, several methods for the synthesis of up-conversion particles exist and are widely used: the thermal decomposition method [15–17], the coprecipitation method [15, 16], and the sol–gel method [15, 18]. The most common method is solvothermal synthesis [18], which is based on the dissolution of inorganic reagents at elevated temperature and pressure, followed by crystal growth from the liquid phase. A special case of this synthesis is the hydrothermal method, in which water serves as a solvent. This synthesis option is widespread due to the simplicity of implementation and the low cost of the starting materials. Moreover, the synthesis in an aqueous medium simplifies the process of surface modification of particles for biomedical applications [15, 19].

In hydrothermal synthesis of up-conversion particles of $NaYF_4$:Er^{3+},Yb^{3+}, various precursors can be used. As a source of rare earth metals Y, Yb, and Er, their salts, for example nitrates or chlorides, may be employed. Various sodium salts are used as a source of sodium: fluoride, citrate (Cit), etc. Sodium fluoride or ammonium fluoride solutions can serve as sources of fluorine [20]. It is worth noting that the reagents can have a double-natured effect. For example, it is known that sodium citrate and sodium fluoride, used as sources of sodium and fluorine ions in the crystal lattice, also affect the crystal growth process itself [20, 21]. This process and the transformation of crystalline phases are affected by the pH of the medium and the amount of an agent (surface modifier) covering surfaces of growth. Crystal surface modifiers are, for example, ethylenediaminetetraacetic acid and abovementioned sodium citrate. Moreover, depending on the pH value, the conditions for blocking the growth of various crystal faces change. As a result, one gets an opportunity, changing the particles' shape from plate to nanorod, to control

E.A. Sagaidachnaya, Ju.G. Konyukhova, N.I. Kazadaeva, A.A. Doronkina, A.A. Skaptsov, A.B. Pravdin Saratov State University, ul. Astrakhanskaya 83, 410012 Saratov, Russia; **I.Yu. Yanina, V.I. Kochubey** Saratov State University, ul. Astrakhanskaya 83, 410012 Saratov, Russia; National Research Tomsk State University, prosp. Lenina 36, 634050 Tomsk, Russia; e-mail: saratov_gu@mail.ru

Received 27 November 2019
Kvantovaya Elektronika **50** (2) 109–113 (2020)
Translated by V.L. Derbov

the morphology of synthesised particles [21]. At the same time, particle surface modifiers are sources of surface ligands that affect the efficiency of up-conversion [22–25].

The results of studies of synthesis factors (parameters) that affect the properties of the obtained up-conversion particles are described in a number of papers [19–23, 26, 27]. However, it should be noted that the synthesis conditions and the ratio of reagent concentrations often differ in the work of different scientific groups. (For example, the synthesis time varies from 1 to 24 hours, the temperature ranges from 160 °C to 220 °C, and the pH of the medium ranges from 3 to 11.) This does not allow us to establish regularities that relate the synthesis conditions to the parameters of the resulting particles.

The aim of this work is to study the effect of the reaction medium pH and fluorinating agent type on the up-conversion luminescence intensity of hydrothermally synthesised β-$NaYF_4:Er^{3+}, Yb^{3+}$ particles of submicron size.

2. Materials and methods

The synthesis of $NaYF_4:Er^{3+}, Yb^{3+}$ particles was carried out according to the following procedure. First, 5.25 g of sodium citrate, $Na_3C_6H_5O_7 \cdot 2H_2O$, was dissolved by stirring in 7.5 mL of distilled water. After 30 min, aqueous solutions of rare-earth metal (Re) salts were added: 0.996 mL of $YCl_3 \cdot 6H_2O$ (0.5 M), 0.212 mL of $YbCl_3 \cdot 4H_2O$ (0.5 M), and 18.6 μL of $ErCl_3 \cdot 5H_2O$ (1 M) (molar ratio Y : Yb : Er = 1 : 0.2 : 0.04). The mixture was stirred for 30 min until the formation of an insoluble metal–citrate complex. The pH of the medium was adjusted with a concentrated solution of HCl or NaOH. Then, 9 mL of 1 M aqueous solution of a fluorinating agent was added. As a fluorine source in the synthesis of the particles, NaF and NH_4F were employed. It should be noted that according to Ref. [28], when using ammonium fluoride in an acidic medium, mainly rod-shaped particles are formed. The molar ratio F : Cit : Re was 14.5 : 28.6 : 1. After stirring for 30 min, the resulting mixture was poured into a Teflon container, which was placed in an autoclave and kept for 2.5 h at a temperature of T = 180 °C. After inertial cooling of the autoclave to room temperature, the obtained particles were separated by centrifugation and washed three times in water. The particles were dried in an air atmosphere at T = 70 °C for 20 h.

Both freshly prepared particles and those annealed at T = 400 °C for one hour in air were investigated. Particles were characterised using electron microscopy, X-ray diffraction (XRD) analysis, luminescence spectroscopy, and Raman scattering. Up-conversion luminescence of powdered samples was recorded using a QE6500 FL luminescence spectrofluorimeter (Ocean Optics, USA) with a fibre input. Luminescence was excited by the radiation of a STLE-M-980-W010 laser diode (λ = 980 nm) with output coupled to an optical fibre. To achieve the repeatable results needed to compare the luminescence intensities of different samples, a fixed amount of dry powder was dispersed in water, and then precipitated upon exposure to weak ultrasound and dried. Thus, close packing of particles in the sample was achieved. Excitation beam formation and luminescence collection were performed by means of 74-VIS collimators (Ocean Optics, USA). The intensity of the exciting radiation was 4 W cm^{-2}. The laser radiation scattered by the sample was suppressed by a SZS-23 filter.

The particle size, shape, and chemical composition were determined using a MIRA 2 LMU scanning electron microscope (TESCAN, Czech Republic).

The structure of the crystal lattice of particles was established using an ARL X'TRA X-ray diffraction system (Thermo Fisher Scientific, USA) and the Jana2006 software. Raman spectra were recorded using a Raman system (Ocean Optics, USA), comprising a QEPRO-RAMAN spectrometer, LASER-785-IP-LAB laser (λ = 785 nm, 1 W power), and RIP-RPB-785-FC probe for Raman spectroscopy. All spectral measurements were carried out at room temperature.

3. Results and discussion

According to electron microscopy, the synthesised $NaYF_4:Er^{3+}, Yb^{3+}$ particles significantly differ in shape (Fig. 1).

As a result of synthesis using sodium fluoride, hexagonal prisms are formed that differ in length and diameter (Fig. 1, samples 1–3, Table 1). The particles are characterised by fairly wide size distributions. Examples of distributions are shown in Fig. 2. At pH = 3, the surface of the particles is defective; in some cases, intergrowths are observed. It should be noted that the visually assessed surface imperfection decreases with increasing synthesis time up to 20 h.

When using ammonium fluoride and a medium with pH = 3, rod-shaped particles with a diameter of $d \approx$ 500 nm and a length of $L \approx$ 5 μm are synthesised (Fig. 1, sample 4, Table 1). At the same time, particles with a diameter $d \approx$ 90 nm and a length $L \approx$ 500 nm are observed.

The ratio of the concentrations of rare-earth elements in the particles is shown in Table 1. According to chemical analysis data obtained by electron microscopy, the relative concentration of ytterbium and erbium in crystals is higher than that in the reaction mixture. This fact can be explained by the different ability of the rare-earth metals used to form citrate complexes.

In the patterns obtained by XRD, the peaks of freshly prepared samples correspond to the hexagonal structure (Fig. 3). To analyse the microstructure of the crystals, Williamson–Hall plots were constructed, from which it follows that the size of the coherent scattering region (CSR) in crystals (Table 1) is significantly smaller than their geometric dimensions. This can be caused by both the defects of crystals (Table 1, microdeformation parameter) and their polycrystallinity. After annealing the samples, the positions of peaks in the XRD patterns did not change, which indicates the persistence of the crystal structure. At the same time, the intensity of the peaks slightly increased, which indicates an increase in the degree of crystallinity of the lattice.

The luminescence spectra of $NaYF_4:Er^{3+}, Yb^{3+}$ particles before and after annealing are shown in Fig. 4. Due to the high luminescence intensity of the particles of sample 4, their spectra are shown in a separate figure. The ratio of luminescence intensities reaches three orders of magnitude. It can be concluded that the highest intensity is observed for the samples synthesised at pH = 3, from which the samples synthesised using ammonium fluoride demonstrate the maximum intensity.

Annealing of the particles leads to an increase in the intensity of their luminescence. This increase differs for different spectral bands and particles obtained under different synthesis conditions. As the ratio of band intensities changes upon annealing, we analysed changes in the integrated luminescence intensity in the range 500–700 nm (Table 1). For the studied particles, there is no correlation between structural data, impurity concentrations, and luminescence intensity.

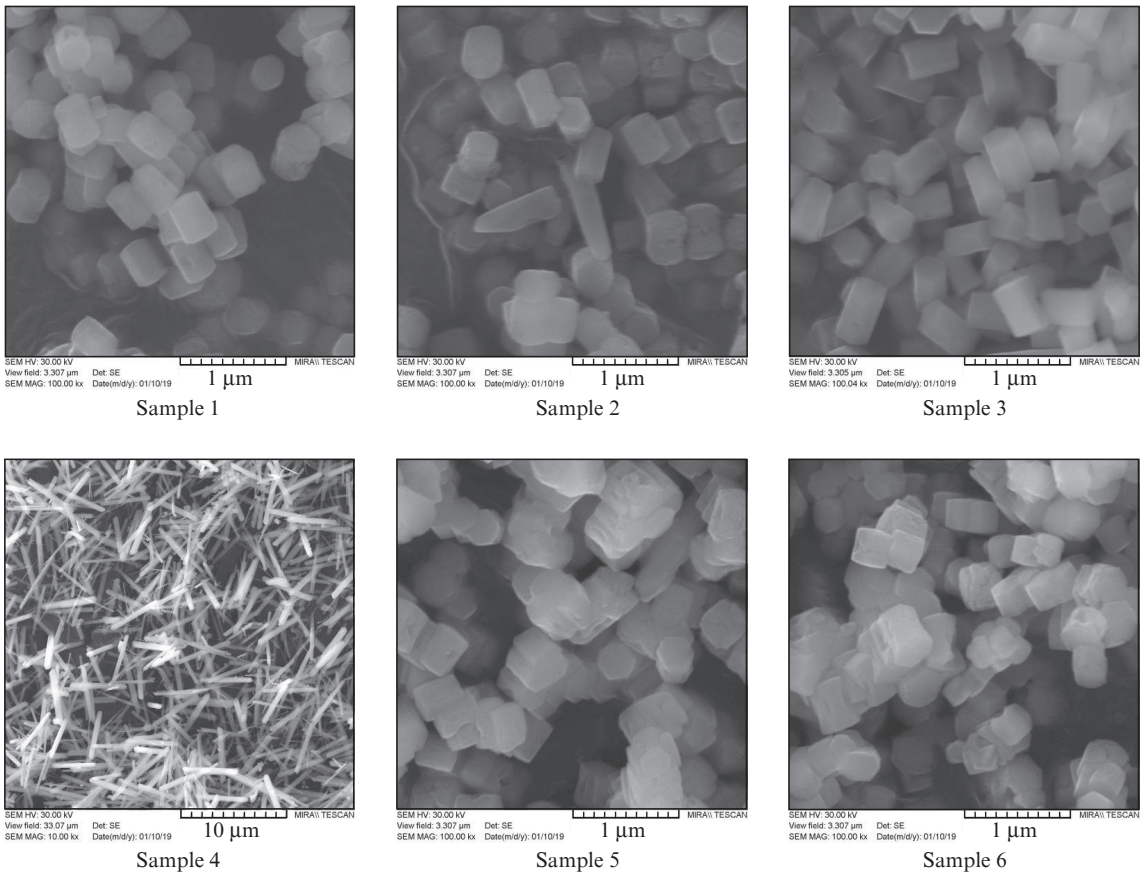

Figure 1. Images of $NaYF_4:Er^{3+},Yb^{3+}$ particles obtained using a scanning electron microscope, for samples 1–6 from Table 1.

Table 1. Characteristics of up-conversion $NaYF_4:Er^{3+},Yb^{3+}$ particles obtained under various synthesis conditions.

Sample number	Fluorinating agent	pH	Length/nm	Diameter/nm	Y:Yb:Er ratio	CSR size /nm	Microdeformation parameter/10^{-3}	Integrated luminescence intensity (arb. units)	
								before annealing	after annealing
1	NaF	8	375 ± 25	310 ± 30	1:0.4:0.06	154	2.7	8.8×10^2	2.2×10^3
2	NaF	10	385 ± 25	310 ± 19	1:0.3:0.05	256	0.4	1.6×10^3	2.1×10^4
3	NaF	3	460 ± 40	315 ± 25	1:0.3:0.03	170	1.5	2.1×10^4	1.2×10^5
4	NH_4F	3	4450 ± 400	480 ± 50	1:0.35:0.05	> 1000	0.9	1.1×10^6	3.9×10^6
5	NH_4F	8	340 ± 20	295 ± 23	1:0.3:0.05	36	0.4	3.5×10^3	1.2×10^5
6	NH_4F	10	280 ± 7	270 ± 14	1:0.35:0.05	45	0.6	6×10^3	3.3×10^4

It is known that quenching by hydroxyl and citrate groups located on the surface of particles affects the intensity of up-conversion luminescence [29]. Particle annealing removes these groups from the surface; however, the degree of removal depends on the annealing temperature: it is maximum at T = 700°C and practically absent at T = 350°C [28, 29]. Citrate groups not only determine the structure of particles and block their growth, forming, under our synthesis conditions, a hexagonal structure, but also block the conversion of the hexagonal structure to cubic upon annealing.

The normalised Raman spectra of unannealed samples are shown in Fig. 5a. The Raman spectra correspond to the β-structure of $NaYF_4$ crystals [30, 31]. In the region ν = 225–450 cm^{-1}, the phonon bands of $NaYF_4$ nanocrystals are located. The weighted average of the phonon modes of the bulk pure $NaYF_4$ single crystal is 360 cm^{-1}, while for nanocrystals doped with Yb and Er it is 304 cm^{-1} [30, 32]. The position of the peaks, i.e., the frequency of phonon vibrations, may alter due to the binding of citrate to the surface; however, for the studied samples the peak positions are the same and do not change upon annealing (Fig. 5b). The Raman spectra of sample 4 are the most intense. This is explained by lower particle defectiveness and better crystallinity [25] and is in good agreement with the XRD data.

In the range ν = 800–1200 cm^{-1}, the spectra of the particles synthesised at pH = 3 contain six bands of different intensities. The nature of these bands is explained in different ways. In particular, it is assumed that the vibrational bands at ν > 500 cm^{-1} relate to vibrations of citrate [32]. According to the authors of Ref. [32], the presence of citrate on the particle surface is indicated by strong bands of non-planar deformation vibrations of COOH in the region of 786–908 cm^{-1} and

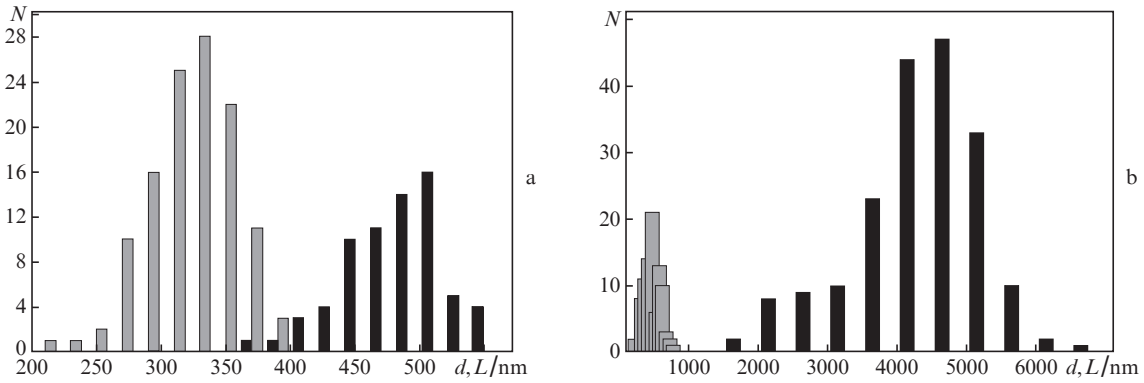

Figure 2. Histograms of the size distribution of the number of particles N for samples (a) 3 and (b) 4. The grey histograms correspond to the distribution over the particle diameter d, the black histograms correspond to the distribution over the particle length L.

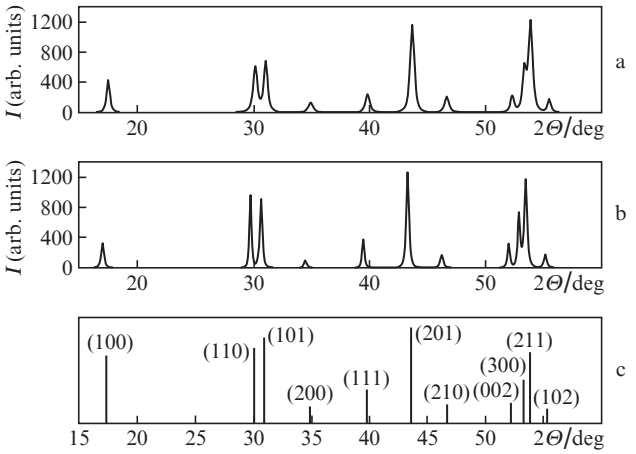

Figure 3. XRD patterns of samples (a) 4 and (b) 3. (c) Arrangement of peaks in the diffraction pattern of the $NaYF_4$ crystal with hexagonal structure.

C–O stretching vibrations in the region of 998–1112 cm^{-1}. But in our case, the absence of a number of bands related to citrate groups, and the fact that the observed bands do not disappear for particles annealed at high temperatures, when citrate groups must be removed from the surface, allow one to doubt this statement.

In Ref. [33], the nature of these bands is analysed both by comparing them with the Raman spectra of other types of crystals and by calculating the vibrational characteristics of the $NaYF_4$ crystal matrix. It was concluded that the presence of bands in the range 750–1500 cm^{-1} cannot be explained by natural vibrations of the lattice of $NaYF_4$ crystal or by the presence of a crystal phase of the Y_2O_3, YOF, or $Y(OH)_3$ type. The authors of Ref. [33] explain the presence of the bands by the existence of hydrolysed surface regions of complex composition, for example, Re–X–OH, where X = O, F.

However, this cannot explain the increase in the intensity of up-conversion luminescence simultaneously with the increase in the intensities of these bands (which we observed in nanoparticles obtained in a number of other syntheses not discussed in this paper, and which is reported in Ref. [34]), because, in the case of nanoparticles, these hydroxyl groups associated with the surface contribute to the transfer of excitation energy to the environment, i.e., they are luminescence

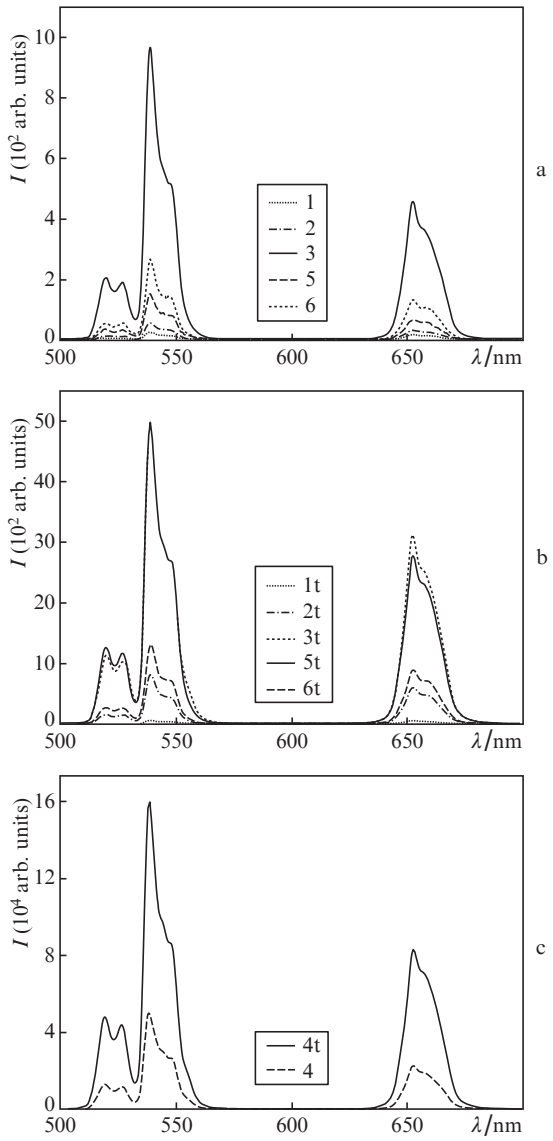

Figure 4. Luminescence spectra of $NaYF_4:Er^{3+},Yb^{3+}$ particles (a) before and (b) after annealing at T = 400°C for one hour. (c) Similar spectra of sample 4 with high luminescence intensity. The figures in the frames are the sample numbers in Table 1, the letter t corresponding to annealed samples (particles).

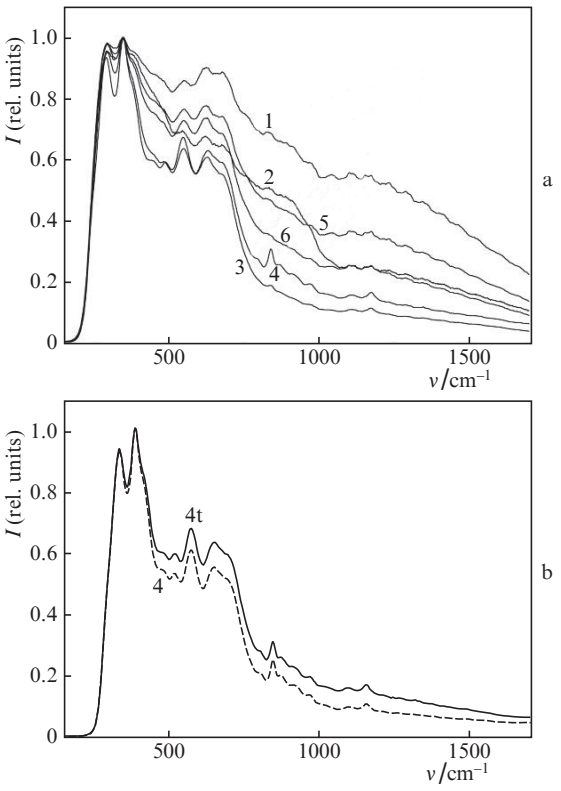

Figure 5. (a) Raman spectra of the samples before annealing and (b) Raman spectra of sample 4 before and after annealing at $T = 400\,^{\circ}C$.

quenchers. Nevertheless, in our case of submicron-size particles, one can expect that, due to the higher value of particle volume to surface area ratio, the effect of hydroxyl groups located on the surface should be small.

4. Conclusions

Thus, according to the obtained results, we can conclude that in order to achieve the maximum luminescence intensity of up-conversion $NaYF_4:Er^{3+},Yb^{3+}$ particles synthesised by the hydrothermal method, it is necessary to use ammonium fluoride and a medium with pH = 3. Under these synthesis conditions, the length of the resulting particles increases, up to the formation of rod-shaped particles. Based on the data on the CSR size and microstresses, we can assume that the particles are polycrystals. At the same time, the limitation of CSR size may be caused by the structural imperfection as well. In the synthesis with pH = 3, hydrolysed regions containing OH groups are formed on the surface of the particles. The presence of these groups, in our opinion, does not affect the intensity of up-conversion luminescence of submicron-size particles.

Acknowledgements. The study was supported by the Russian Science Foundation (Project No. 19-12-00118).

References

1. Chen G., Qiu H., Prasad P.N., Chen X. *Chem. Rev.*, **114**, 5161 (2014).
2. Wang F., Banerjee D., Liu Y., Chen X., Liu X. *Analyst*, **135**, 1839 (2010).
3. Eliseeva S.V., Bünzli J.-C.G. *Chem. Soc. Rev.*, **39**, 189 (2010).
4. Jafari M., Rezvanpour A. *Adv. Powder Technol.*, **30**, 1731 (2019).
5. Del Rosa B., Jaque D. *Methods Appl. Fluoresc.*, **7**, 022001 (2019).
6. Fan Y., Liu L., Zhang F. *Nano Today*, **25**, 68 (2019).
7. Li X., Zhang F., Zhao D. *Chem. Soc. Rev.*, **44**, 1346 (2015).
8. DaCosta M.V., Doughan S., Han Y., Krull U.J. *Anal. Chim. Acta.*, **832**, 1 (2014).
9. Tessitore G., Mandl G.A., Brik M.G., Parke W., Capobianco J.A. *Nanoscale*, **11** (25), 12015 (2019).
10. Sun M., Dong H., Dougherty A.W., Lu Q., Peng D., Wong W.-T., Huang B., Sun L.-D., Yan C.-H. *Nano Energy*, **56**, 473 (2019).
11. Yi G.S., Chow G.M. *Adv. Funct. Mater.*, **16**, 2324 (2006).
12. Kaiser M., Würth C., Kraft M., Soukka T., Resch-Genger U. *Nano Res.*, **12**, 1871 (2019).
13. Rafique R., Baek S.H., Tu Phan L.M., Chang S.-J., Gul A.R., Park T.J. *Mater. Sci. Eng. C*, **99**, 1067 (2019).
14. Podhorodecki A., Banski M., Noculak A., Sojka B., Pawlik G., Misiewicz J. *Nanoscale*, **5**, 429 (2013).
15. Chang H., Xie J., Zhao B., Liu B., Xu S., Ren N., Xie X., Huang L., Huang W. *Nanomaterials*, **5**, 1 (2015).
16. Gainer C.F., Romanowski M. *J. Innovative Opt. Health Sci.*, **7**, 1330007 (2014).
17. Chen J., Zhao J.X. *Sensors*, **12**, 2414 (2012).
18. Zhang F. *Photon Upconversion Nanomaterials* (London–New York: Springer, 2016).
19. Zhao J., Zhao J., Sun Y., Kong X., Tian L., Wang Y., Tu L., Zhao J., Zhang H. *J. Phys. Chem. B*, **112**, 15666 (2008).
20. Li C., Yang J., Quan Z., Yang P., Kong D., Lin J. *Chem. Mater.*, **19**, 4933 (2007).
21. Zhang X., Yu H., Guo L., Jin J., Li Q., Guo Y., Fu Y., Shi Y., Zhao L. *J. Alloys Compd.*, **728**, 1254 (2017).
22. Li C., Quan Z., Yang J., Yang P., Lin J. *Inorg. Chem.*, **46**, 6329 (2007).
23. Zhou J., Liu Q., Feng W., Sun Y., Li F. *Chem. Rev.*, **115**, 395 (2015).
24. Liu X., Deng R., Zhang Y., Wang Yu., Chang H., Huang L., Liu X. *Chem. Soc. Rev.*, **44**, 1479 (2015).
25. Altavilla C. (Ed.) *Upconverting Nanomaterials: Perspectives, Synthesis, and Applications. Series: Nanomaterials and their Applications* (Boca Raton: Taylor & Francis, 2016).
26. Shang Y., Hao S., Liu J., Tan M., Wang N., Yang C., Chen G. *Nanomaterials*, **5**, 218 (2015).
27. Ding M., Yin S., Ni Y., Lu C., Chen D., Zhong J., Ji Z., Xu Z. *Ceram. Int.*, **41**, 77411 (2015).
28. Zhao J.W., Jia T.K., Kong X.G. *Adv. Mater. Res.*, **496**, 79 (2012).
29. Chunxia Li, Jun Yang, Zewei Quan, Piaoping Yang, Deyan Kong, Jun Lin. *Chem. Mater.*, **19**, 4933 (2007).
30. Wang F., Wang J., Liu X.G. *Angew Chem. Int. Ed.*, **49**, 7456 (2010).
31. Wilhelm S., Hirsch T., Patterson W.M., Scheucher E., Mayr T., Wolfbeis O.S. *Theranostics*, **3**, 239 (2013).
32. Klier D.T., Kumke M.U. *J. Mater. Chem. C*, **3**, 11228 (2015).
33. Du Y. PhD thesis (Department of Materials Science & Engineering National University of Singapore, 2012).
34. Suyver J.F., Grimm J., Van Veen M.K., Biner D., Krämer K.W., Güdel H.U. *J. Lumin.*, **117**, 1 (2006).